SEASONAL/DIURNAL MAPPING OF OZONE AND WATER IN THE MARTIAN ATMOSPHERE.

R. E. Novak[1], M. J. Mumma[2], M. A. DiSanti[2], N. Dello Russo[3], K. Magee-Sauer[4], B. Bonev[5], [1]Iona College, New Rochelle, NY 10801-1830, rnovak@iona.edu, [2]NASA/GSFC, Greenbelt, MD 20771-0003, [3]Catholic University of American, Washington DC 20064-0001 and NASA/GSFC, Greenbelt, MD 20771-0003, [4]Rowan University, Glassboro, NJ 08028-1702, [5]Ritter Astrophys. Res. Ctr., University of Toledo, Toledo OH 43606

Introduction: Ozone and water are key species for understanding the stability and evolution of Mars' atmosphere; they are closely linked (along with CO, H, OH, and O) through photochemistry [1-4]. Photolysis of water produces the OH radical (thought to catalyze reformation of CO_2 from CO and O_2) and atomic hydrogen (which reacts with O_3 forming OH and O_2). Atomic hydrogen also reacts with O_2 (forming HO_2), thereby reducing the amount of O_2 available to reform O_3 from collisions between O and O_2. Hence ozone and water should be anti-correlated on Mars.

Photolysis of O_3 produces $O_2(a^1\Delta_g)$ with 90% efficiency [5], and the resulting emission band system near 1.27 μm traces the presence and abundance of ozone. This approach was initially used to study ozone on Earth [6] and then applied to Mars [7]. In 1997, we measured several lines of the $O_2(a^1\Delta_g)$ emission (Fig. 1.) using CSHELL [8] at the NASA IRTF; the $O_2(a^1\Delta_g)$ state is also quenched by collisions with CO_2. This quenching dominates at lower altitudes so that the detected emissions are used to detect ozone column densities above ~20 km. The slit was positioned N-S along Mars' central meridian resulting in a one-dimensional map of ozone [9].

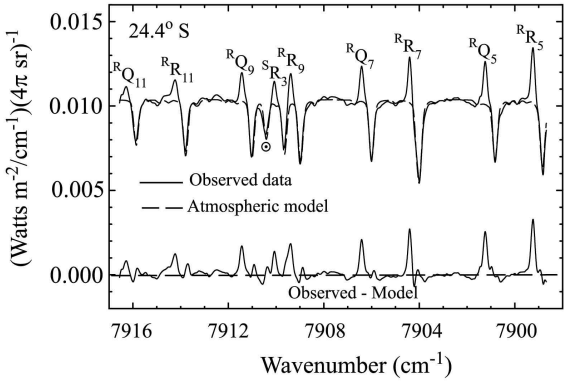

Fig. 1. Spectral extract (summed over one arc-second) on Mars centered at 24.4° S latitude, 2:20 PM local time on Jan 21, 1997 (L_s = 67°). The continuum is sunlight reflected from Mars' surface. Emission lines from the O_2 ($a^1\Delta_g$) state are labeled. The synthetic terrestrial atmospheric model is indicated by the dashed trace. The difference between the observed spectrum and the atmospheric model reveals the isolated O_2 ($a^1\Delta_g \rightarrow X^3\Sigma_g$) emission from Mars' atmosphere (lower trace). A Boltzmann analysis of the emission lines determines a rotational temperature (175 +/- 5 K), and the column density above ~20 km (2.8 +/- 0.2 μm-atm) [9].

Nearly simultaneous maps may be made of water using CSHELL by detecting the n_1 fundamental band of HDO near 3.67 μm (Fig. 2) and using the D/H ratio for Mars [10]. This technique was used by DiSanti and Mumma [11]. With CSHELL, measurements for both $O_2(a^1\Delta_g)$ emissions and HDO absorptions can be made during the day or night.

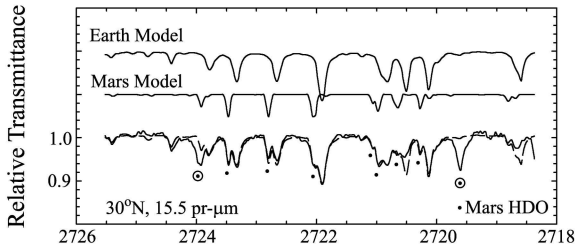

Fig. 2. Detection of HDO on Mars Jan 21, 1997 (L_s = 67.3°). The observed spectral trace (solid curve-bottom plot) is an extract summed over 1.0 arc-sec on Mars. The upper traces are atmospheric transmittance models generated for the Earth and Mars (Doppler-shifted); these are combined and plotted as the dashed trace with the observed spectrum. The best fit between the HDO lines of the observed spectrum (indicated by dots) and the convolved model provides the column abundance of water on Mars. A D/H ratio of 5.2 times the standard mean ocean water ratio was adopted [10]. Solar Fraunhofer lines are also detected [9].

Since January, 1997, we have repeated these measurements at different times during the Martian year (Table I). For all of these dates, we have positioned the slit N-S along the central meridian; for some of these dates, we have also stepped the slit across the planet at 1 arc-sec intervals generating a 2-dimensional map. We have also positioned the slit E-W on Mars thus providing diurnal variations of ozone and water along the slit.

Seasonal Variation of Ozone and Water: A summary of our observations taken at four different times during the Martian year appears in Fig. 3. The largest measured column density of ozone appears near

aphelion (L_s = 67°). The measured ozone (column density above 20 km) is large in both hemispheres, but is not seen to be anti-correlated with the measured water density. Furthermore, a decrease in the measured ozone level appears near the sub-solar (23.5° N) location. Our measurements of ozone were taken close in time to those taken with the Faint Object Spectrometer (FOS) on the Hubble Space Telescope [12]; this instrument measures the total column density of ozone. The CSHELL measurements [9] are consistently smaller than the FOS measurements. The CSHELL measurements also vary smoothly from south to north whereas the FOS measurement show a wider variation in values; the CSHELL measurements have a field of view of ~ 1 arc-sec causing localized variations to average out while the FOS measurements have better spatial resolution on Mars. We believe that both measurements are consistent as explained by an atmospheric model for near-aphelion conditions [13]. Near-aphelion, water vapor is located at altitudes < 10 km; at altitudes above 20 km, water vapor is small and would not affect the ozone density. Since we measure ozone above 20 km, we interpret our ozone measurements to be insensitive to the water measurements located at lower altitudes.

For the L_s=67° measurements, the decrease in ozone density near the sub-solar point has not been sufficiently explained; during this season, ice clouds at mid-latitudes could affect the density of ozone. Another explanation is that the ice clouds prevent some of the ozone from being photolyzed causing a smaller emission from the $O_2(a^1\Delta_g)$ state [14]. This phenomenon requires further analysis.

The measurements at L_s=103° and L_s=133° show a decrease of ozone in the northern hemisphere with the ozone being concentrated in the southern hemisphere during the late northern summer; at this time, the water column density in the north reaches its yearly maximum [15]; also, the water vapor probably extends to higher altitudes causing the ozone level to decrease. This seasonal decrease is not as drastic in the southern hemisphere since the overall water column density there is still relatively low.

Observations taken during early northern winter (L_s=306°) show no detectable emissions from the $O_2(a^1\Delta_g)$ state across most of the planet indicating a reduced value of ozone above 20 km. This may be explained using a model for near perihelion conditions [13]. At this season, water vapor extends to higher altitude than at aphelion causing a reduction of ozone above 20 km. Though the water column density in the northern hemisphere is smaller at this time than at L_s=67°, its location at a higher altitude reduces ozone above 20 km.

TABLE I
CSHELL Observations of Mars

UT date	L_s	Del-Dot (km sec^{-1})	Diameter
21 Jan 1997	67°	-15.3	9.6"
01 Mar 1997	84°	-7.2	13.4"
20 Mar 1999	112°	-12.7	12.6"
05 Jul 1999	165°	10.5	11.1"
15 Jan 2001	103°	-17.0	5.7"
20 Mar 2001	133°	-16.5	9.2"
10 Jan 2002	306°	13.0	6.0"
13 Jan 2003	124°	-14.9	4.8"
21 Mar 2003	154°	-15.6	6.9"

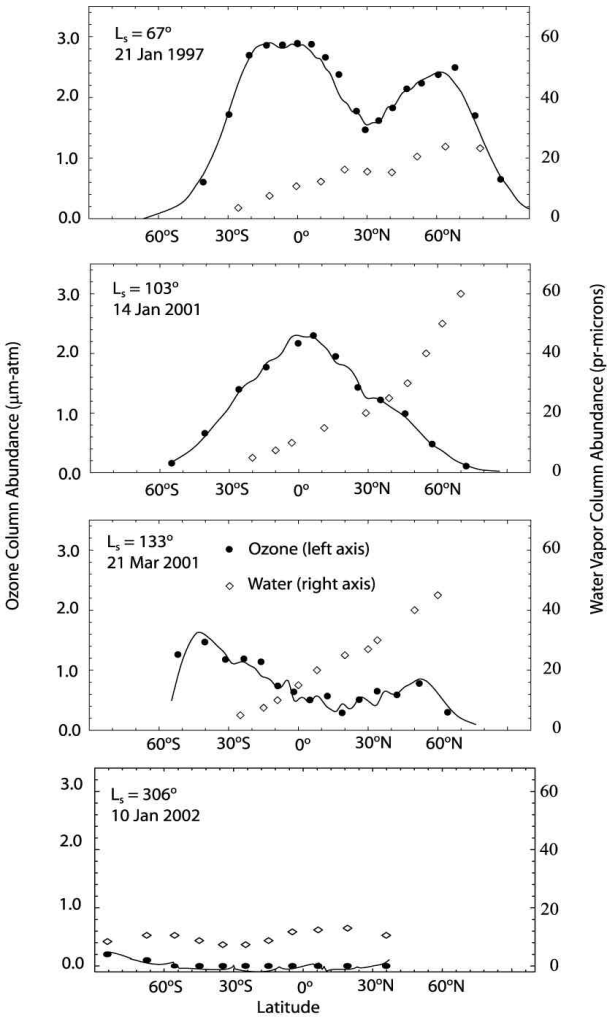

Fig. 3. Water and ozone maps taken at different times during Mars' year using CSHELL. The water measurements are taken by measuring HDO spectra on Mars and using a D/H ratio of 5.2 to obtain water column densities [10]. The data indicate that the relationship between water and ozone also depends on altitude.

A better explanation for the relationship between water and ozone in the Martian atmosphere requires vertical profiles of both molecules; to date, detailed measured profiles are lacking. Our CSHELL measurements provide limited but useful vertical profile information when combined with measurements of the total column density of ozone from space [12] or ground based [16] observations. We plan to determine an "average" altitude for water by performing a Boltzmann analysis on Mars HDO absorption lines (Fig. 4). The retrieved rotational temperature can be compared to altitude profiles of temperature obtained from MGS-TES measurements [15].

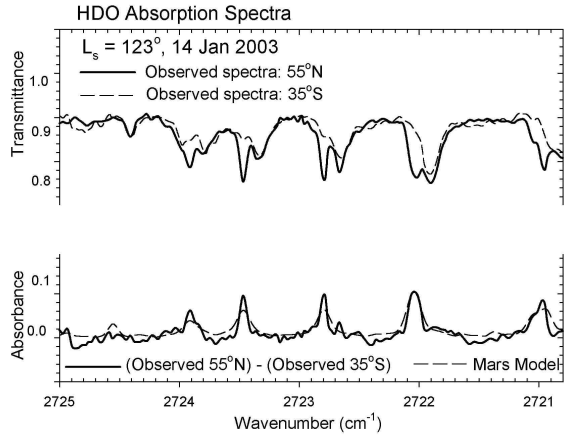

Fig. 4. HDO absorption spectra. Top traces show observations at different latitudes; bottom trace shows difference between the two, canceling the earth's atmosphere and yielding the difference in water column density between the two latitudes.

Diurnal Variation of Ozone: In additional to seasonal effects, ozone is expected to show strong diurnal variation; CSHELL measurements confirm this (Fig. 5). These data were taken with the slit oriented parallel to the equator of Mars and centered at 57°S; the sub-earth point corresponds to 2:00 PM local time. The presented Mars emissions are taken at equal air-masses (1.6 arc-sec either side (11:00 AM and 5:00 PM) of the sub-earth point); the decrease in emission intensity indicates a decrease in ozone towards late afternoon; the observed terminator was in the evening sky. Ozone is regenerated during the night ($O + O_2 + M \rightarrow O_3 + M$; $OH + O_2 \rightarrow H + O_3$), and a measure near dawn will permit an assessment of this production. Observing the morning terminator, which is available after apparition, will enable us to measure the regenerated ozone and to follow its photolysis through late afternoon.

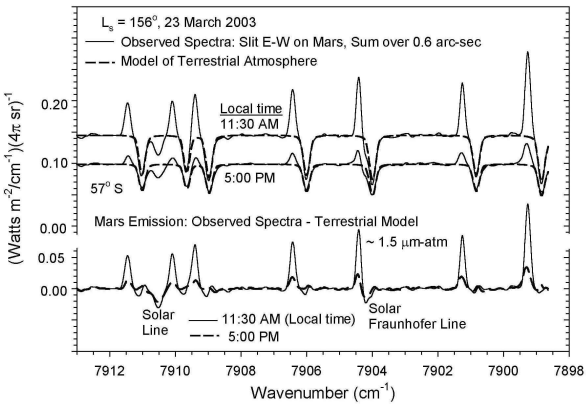

Fig. 5. Observed spectra (O_2 ($^1\Delta$) emissions) taken with the slit E-W on Mars and centered at 57°S. The two observed spectra are 1.6 arc-sec either side of the sub-earth points (11:00 AM, 5:00 PM local time). A terrestrial model is subtracted from the observed spectra yielding O_2 ($^1\Delta_g$) emission lines in the Mars spectra that are Doppler shifted from the corresponding earth absorptions. Decrease in the $O_2(^1\Delta_g)$ emission through the day results from photodestruction of ozone by the UV Hartley band.

Future Plans: Our goal is to take observations throughout the entire Martian year. Mars' eccentric orbit leads to ~45% more insolation at perihelion than aphelion; this results in the large difference between northern summer and southern summer as shown by data taken at L_s = 103° and L_s = 306° in Fig. 3. Our observations require Doppler shifts greater than 10 km sec^{-1} in order to distinguish Mars' spectra from the earth's. Seasonal gaps in our database exist between L_s = 165° and L_s = 306° and between L_s = 306° and L_s = 67° ; during the time period of the latter gap, the ozone column density is expected to increase drastically across the planet. January – April, 2004 will provide the opportunity to observe Mars between L_s = 330° and L_s = 10°. Continued mapping with the slit E-W will provide information on both the photodestruction and the regeneration of ozone above 20 km.

Acknowledgments: This work was supported in part by grants from NASA (RTOP 693-344-32-31) and the NSF (AST-0205397). Data presented herein were obtained at the NASA Infrared Telescope Facility (IRTF), which is operated for NASA by the University of Hawaii. We gratefully acknowledge the support of the IRTF Director and the expert assistance of the IRTF telescope operators and staff.

References: [1] Hunten, D. M. (1974) *Rev. Geophys. Space Phy. 12*, 529-535. [2] Krasnopolsky, V.A. (1993) *Icarus 101*, 313-332. [3] Nair, H., et al. (1994) *Icarus 111*, 124-150. [4] Yung, Y.L. and W. B. DeMore (1999) *Photochemistry of Planetary Atmos-*

pheres, Oxford University Press, New York. [5] Ball, S.M. et al. (1993) *Geophys. Res. Let. 20*, 2063-2066. [6] Noxon, J.F. (1968). *Sp. Sci. Rev. 8*,92-134. [7] Noxon et al. (1976) *Ap. J. 207*,1025-1035. [8] Tokunaga, A. T et al.*Proc. SPIE 1235*, 131-143. [9] Novak, R. E. et al. (2002), *Icarus 158*, 14-23. [10] Bjoraker, G. L. et al. (1989) *B.A.A.S. 21*, 991. [11] DiSanti, M.A. and M.J. Mumma (1995) *Workshop on Mars Telescope Observations* (Cornell U. Press). [12] Clancy, R. T., et al. (1999) *Icarus 138*, 49-63. [13] Clancy, R.T. and H. Nair (1996) *J. Geophys. Res. 101(E5)*, 12785-12790. [14] Pearl, J.C. et al. (2001) *J. Geophys. Res. 106*, 12325-12338. [15] Smith, M.D. (2001) *J. Geophys. Res. 106*, 23929-12945. [16] Espenak, F. et al. (1991), *Icarus 92*, 242-262.